A sharp interface in-cell-reconstruction method for volume tracking phase interfaces in compressible flows

By M. Herrmann†

We present a hybrid capturing/tracking method (Smiljanovski *et al.* 1997) for compressible multiphase flows that couples an unsplit geometric volume tracking method (Owkes & Desjardins 2014) with a finite volume wave propagation scheme (LeVeque 2010). In cells containing the phase interface, states on either side of the interface are reconstructed such that the cell-face Riemann problems can be solved within each phase separately. Using area-fraction-weighted single-phase fluxes together with a linearization of the wave interaction across cell faces avoids the small cut-cell time step limitation of typical tracking methods. The interaction of waves with the phase interface is solved using an exact two-phase Riemann solver with arbitrary jumps in the equation of state. Several test cases highlight the capabilities of the new method.

1. Introduction

To accurately predict the interaction of phase interfaces with shocks and rarefaction waves, sharp interface methods that maintain the phase interface as a discontinuity are preferable to capturing methods that tend to smear the interface due to dissipative errors, generating non-physical intermediate states in an interface zone.

Numerous numerical approaches that maintain the phase interface as a discontinuity, among them explicit geometric interface tracking methods (Chern *et al.* 1986) and level set approaches employing the ghost fluid method (Fedkiw *et al.* 1999), have been developed in the past. A summary of recent numerical methods is given, for example, in Jemison *et al.* (2014).

The drawback of most of these sharp interface methods is that they either have to sacrifice conservative formulations locally at the interface and/or require a small cut-cell treatment using, for example, mixing rules (Hu *et al.* 2006). In this report we present a sharp interface approach that avoids both of these potential drawbacks. Our method is based on the hybrid capturing/tracking method developed for deflagration waves (Smiljanovski *et al.* 1997), extending the method to two-phase flows using a geometric volume-of-fluid (VoF) method to localize the phase interface. While VoF-based compressible approaches have been proposed in the past, see, for example, Shyue (1999) and the ghost fluid method of Bo & Grove (2014), the advantage of the method proposed here is that it builds upon a standard finite volume formulation, enforces local conservation, and avoids the small cut-cell problem by updating finite volume averaged quantities directly.

† School for Engineering of Matter, Transport and Energy, Arizona State University

2. Governing equations

The governing equations describing compressible flows are the Navier-Stokes equations. For simplicity, we will focus here on the inviscid limit only; hence, the flow is governed by the Euler equations,

$$\frac{\partial}{\partial t}\begin{bmatrix}\rho\\ \rho u\\ \rho v\\ \rho w\\ \rho E\end{bmatrix}+\frac{\partial}{\partial x}\begin{bmatrix}\rho u\\ p+\rho u^2\\ \rho uv\\ \rho uw\\ u(\rho E+p)\end{bmatrix}+\frac{\partial}{\partial y}\begin{bmatrix}\rho v\\ \rho uv\\ p+\rho v^2\\ \rho vw\\ v(\rho E+p)\end{bmatrix}+\frac{\partial}{\partial z}\begin{bmatrix}\rho w\\ \rho uw\\ \rho vw\\ p+\rho w^2\\ w(\rho E+p)\end{bmatrix}=0\,. \tag{2.1}$$

Here ρ is the density, u, v, and w are the velocity components in the three spatial directions, p is the pressure, and E is the specific total energy, defined as

$$\rho E=\rho i+\frac{1}{2}\rho q^2\,, \tag{2.2}$$

with i as the specific internal energy and $q^2=u^2+v^2+w^2$. The above system of equations is closed by an equation of state, $p=p(\rho,i)$. Here, we use a stiffened equation of state,

$$p=(\gamma-1)\rho i-\gamma p_\infty\,, \tag{2.3}$$

where γ and p_∞ are modeling parameters specific to the fluid of interest. For ideal gases, $p_\infty=0$ and γ is the ratio of specific heats, reverting Eq. (2.3) to the ideal gas law. From Eq. (2.3) it follows that the speed-of-sound c is

$$c=\sqrt{\gamma\frac{p+p_\infty}{\rho}}. \tag{2.4}$$

In the continuum limit, the liquid/gas interface Γ is a discontinuity, resulting in the following jump conditions across the interface,

$$[\![u]\!]_\Gamma=0,\quad [\![v]\!]_\Gamma=0,\quad [\![w]\!]_\Gamma=0,\quad [\![p]\!]_\Gamma=\sigma\kappa, \tag{2.5}$$

where σ is the surface tension coefficient and κ is the interface curvature. The above jump conditions are compatible with the Euler equations; i.e., the temperature T (Menikoff 2007),

$$T=\frac{p+p_\infty}{(\gamma-1)c_v\rho}, \tag{2.6}$$

where c_v is the specific heat at constant volume, may have an arbitrary jump across the phase interface.

In compressible flows, the location of the interface Γ is usually captured by a level set method (Hu *et al.* 2006) or an interface marker tracking method (Bo *et al.* 2011; Terashima & Tryggvason 2009). Here, we propose to use a VoF method. VoF methods have proven highly successful in capturing interfaces in incompressible flows, since they can be constructed to conserve volume exactly, an essential feature in incompressible flows, as fluid volume is a conserved quantity there. However, fluid volume is not conserved in the compressible limit. The choice of a VoF method is thus driven by geometric considerations as outlined below. In the VoF method, the liquid fluid volume is given by the solution of

$$\frac{\partial\alpha}{\partial t}+\nabla\cdot(\vec{v}\alpha)=\alpha\nabla\cdot\vec{v}, \tag{2.7}$$

where $\vec{v}=(u,v,w)^T$ is the velocity vector.

3. Numerical methods

The Euler equations (2.1) are solved using the second-order wave distribution algorithm of LeVeque (2010). When a finite volume method is used, each control volume Ω_{cv} stores the volume average of the conservative variables $\vec{Q} = (\rho, \rho u, \rho v, \rho w, \rho E)^T$,

$$\vec{Q}_{cv} = \frac{1}{V_{cv}} \int_{\Omega_{cv}} \vec{Q}(\vec{x}) d\vec{x}, \tag{3.1}$$

where V_{cv} is the volume of Ω_{cv}. Following a Godunov approach, local cell-face Riemann problems can be defined using as left and right states the control volume averages of $\vec{Q}$ in the two cells sharing the face, i.e., $\vec{Q}^L_{cv}$ and $\vec{Q}^R_{cv}$. The cell-face Riemann problems are linearized using Roe averages (Roe 1981; Glaister 1988), decomposed into waves $\mathcal{W}^p$ with wave speeds λ^p, resulting in left- and right-going fluctuations $\mathcal{A}^{\pm}\Delta\vec{Q}$ (LeVeque 2010),

$$\mathcal{A}^{\pm}\Delta\vec{Q} = \sum_p (\lambda^p)^{pm} \mathcal{W}^p, \tag{3.2}$$

that are subjected to the entropy fix by Harten & Hyman (1983). To achieve second-order accuracy in space, correction fluxes are calculated by comparing projections of neighboring cell-face waves to each other (LeVeque 2010) using the monotonized central-difference limiter (MC limiter) of van Leer (1977). In two and three dimensions, we use either a dimensionally split version of the wave distribution algorithm using Godunov splitting (LeVeque 2010) or an un-split version that solves additional transverse Riemann problems in the cell-face tangential directions for the fluctuations (Langseth & LeVeque 2000).

The solution algorithm described so far is applicable only if neither control volume adjacent to the cell face of interest contains the phase interface; i.e., both the left and right states of the Riemann problem $\vec{Q}^L_{cv}$ and $\vec{Q}^R_{cv}$ are the respective pure liquid and gas states. However, should either of the cells contain the interface, the cell-face Riemann problem involves phase averaged states, resulting in a non-sharp interface treatment. We address this issue by an in-cell-reconstruction technique first introduced by Smiljanovski (1996) and Smiljanovski *et al.* (1997) for deflagration waves. The extension of this technique to phase interfaces is described in the following subsections.

3.1. *In-cell-reconstruction for phase interfaces*

The goal of the in-cell-reconstruction scheme (Smiljanovski 1996; Smiljanovski *et al.* 1997) is to avoid mixed-phase Riemann problems and build the solution from Riemann problems that are purely in the gas and the liquid. Let $\vec{Q}_1$ and $\vec{Q}_0$ be the respective pure liquid and gas states in the control volume Ω_{cv} containing the phase interface, then following Eq. (3.1),

$$\vec{Q}_{cv} = \frac{1}{V_{cv}} \int_{\Omega_{cv}} \vec{Q}(\vec{x}) d\vec{x} = \frac{1}{V_{cv}} \left(\int_{\Omega_1} \vec{Q}_1(\vec{x}) d\vec{x} + \int_{\Omega_0} \vec{Q}_0(\vec{x}) d\vec{x} \right) \tag{3.3}$$

where Ω_1 and Ω_0 are the liquid respective gas volumes in the control volume with $\Omega_{cv} = \Omega_1 + \Omega_0$. Applying Eq. (3.1) to each of the volume integrals results in

$$\vec{Q}_{cv} = \alpha \vec{Q}_{cv,1} + (1-\alpha)\vec{Q}_{cv,0}, \tag{3.4}$$

where α is the volume fraction of the control volume that is liquid and $\vec{Q}_{cv,1}$ and $\vec{Q}_{cv,0}$ are the cell averages over the cell volume fractions occupied by their respective phases. As shown in Figure 1, if one were able to reconstruct the pure liquid and gas states $\vec{Q}_{cv,1}$

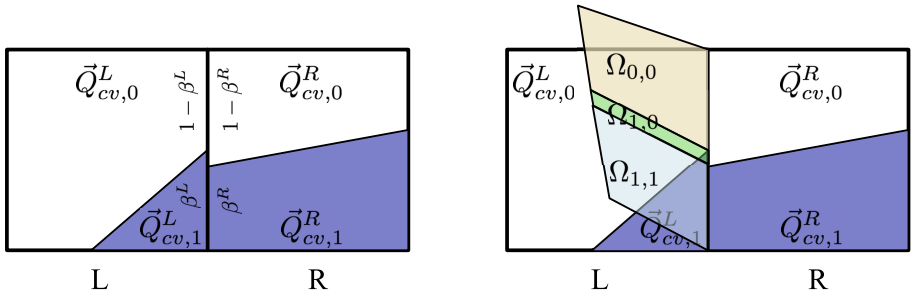

FIGURE 1. Cell-face Riemann problems using reconstructed states (left) and interface wave flux volumes (right).

and $\vec{Q}_{cv,0}$ from the known cell average $\vec{Q}_{cv}$, one could solve cell-face Riemann problems in either phase separately using the approach described in the prior section.

To derive the equations for reconstruction, we combine Eq. (3.4) with the jump conditions across the phase interface, Eq. (2.5), resulting in a system of 9 equations for the 10 unknowns. The system is underdetermined because in the context of the Euler equations the phase interface may have an arbitrary jump in temperature. Note that in the context of the Navier-Stokes equations, the jump in temperature has to be zero, $[\![T]\!]_\Gamma = 0$.

Using this zero temperature jump for the Euler equations also results in the following equations, reconstructing the primitive variables from the conservative cell averaged states indicated by an overline,

$$
\begin{aligned}
u_0 &= u_1 = \frac{\overline{\rho u}}{\overline{\rho}}, \quad v_0 = v_1 = \frac{\overline{\rho v}}{\overline{\rho}}, \quad w_0 = w_1 = \frac{\overline{\rho w}}{\overline{\rho}} \\
p_0 &= \frac{(\gamma_0-1)(\gamma_1-1)\left(\overline{\rho E} - \frac{1}{2}q^2\right) - \alpha(\gamma_0-1)(\sigma\kappa+\gamma_1 p_{1,\infty}) - (1-\alpha)(\gamma_1-1)\gamma_0 p_{0,\infty}}{\alpha(\gamma_0-1)+(1-\alpha)(\gamma_1-1)} \\
p_1 &= p_0 + \sigma\kappa \\
\rho_0 &= \frac{(p_0+p_{0,\infty})(\gamma_1-1)c_{v,1}\overline{\rho}}{\alpha(p_1+p_{1,\infty})(\gamma_0-1)c_{v_0} + (1-\alpha)(p_0+p_{0,\infty})(\gamma_1-1)c_{v_1}} \\
\rho_1 &= \frac{(p_1+p_{1,\infty})(\gamma_0-1)c_{v,0}\overline{\rho}}{\alpha(p_1+p_{1,\infty})(\gamma_0-1)c_{v_0} + (1-\alpha)(p_0+p_{0,\infty})(\gamma_1-1)c_{v_1}},
\end{aligned}
\tag{3.5}
$$

with $q^2 = u_0^2+v_0^2+w_0^2 = u_1^2+v_1^2+w_1^2$.

To replace $[\![T]\!]_\Gamma = 0$, we propose to minimize the square of the sum of the temperature differences between the reconstructed pure liquid and gas states and their respective neighbor cells T_1^n and T_0^n. Starting from the gas side, this results in the following nonlinear equation for the temperature difference $\epsilon_0 = T_0^n - T_0$,

$$
\frac{d}{d\epsilon_0}\left[\epsilon_0^2 + \left(\frac{p_1+p_{1,\infty}}{(\gamma_1-1)c_{v_1}}\frac{\alpha(\gamma_0-1)c_{v_0}(T_0^n+\epsilon_0)}{\overline{\rho}(\gamma_0-1)c_{v_0}(T_0^n+\epsilon_0) - (1-\alpha)(p_0+p_{0,\infty})} - T_1^n\right)^2\right] = 0. \tag{3.6}
$$

Starting from the liquid side, the following equation is obtained for $\epsilon_1 = T_1^n - T_1$,

$$
\frac{d}{d\epsilon_1}\left[\epsilon_1^2 + \left(\frac{p_0+p_{0,\infty}}{(\gamma_0-1)c_{v_0}}\frac{(1-\alpha)(\gamma_1-1)c_{v_1}(T_1^n+\epsilon_1)}{\overline{\rho}(\gamma_1-1)c_{v_1}(T_1^n+\epsilon_1) - \alpha(p_1+p_{1,\infty})} - T_0^n\right)^2\right] = 0\,. \tag{3.7}
$$

The above two equations can be solved after taking the exact derivative using a pro-

gression of a standard Newton root finder and the zeroin method (Grund 1979). Using Eq. (3.6) together with Eq. (2.6) yields

$$\rho_0 = \frac{p_0 + p_{0,\infty}}{(\gamma_0 - 1)c_{v_0}(T_0^n + \epsilon_0)}, \quad \rho_1 = \frac{\overline{\rho} - (1-\alpha)\rho_0}{\alpha}, \tag{3.8}$$

whereas using Eqs. (3.7) and (2.6) results in

$$\rho_1 = \frac{p_1 + p_{1,\infty}}{(\gamma_1 - 1)c_{v_1}(T_1^n + \epsilon_1)}, \quad \rho_0 = \frac{\overline{\rho} - \alpha\rho_1}{1-\alpha}. \tag{3.9}$$

Since Eq. (3.8) contains a division by α that is problematic for small α, and Eq. (3.9) contains a division by $1-\alpha$, problematic for α close to 1, we use Eqs. (3.6) and (3.8) for mixed cells, with $\alpha \geq 0.5$, and Eqs. (3.7) and (3.9) for mixed cells, with $\alpha < 0.5$.

Finally, using the reconstructed liquid and gas primitive variables, the reconstructed conservative variables in both the liquid and gas, $\vec{Q}_{cv,1}$ and $\vec{Q}_{cv,0}$, can be calculated.

3.2. *Mixed cell updates*

Using the reconstructed liquid and gas states in mixed cells, cell-face Riemann problems that are solely within single phases can be constructed and solved. However, using the fluctuations from these Riemann problems to update the reconstructed states associated with the liquid cell volume $\alpha\Omega_{cv}$ and the gas cell volume $(1-\alpha)\Omega_{cv}$ directly would result in a small cut-cell time step limitation that is prohibitive, since α can be arbitrarily close to 0 or 1, and hence the associated volumes can be arbitrarily small. Instead, following the ideas by Smiljanovski (1996); Smiljanovski *et al.* (1997), we update only the cell averaged mixed state $\vec{Q}_{cv}$.

To calculate the required averaged fluctuations for each face intersected by the interface, the individual pure gas and liquid fluctuations resulting from the pure-phase Riemann problems are averaged using the liquid cell-face area fraction β,

$$\mathcal{A}^{\pm}\Delta\vec{Q}_{cv} = \beta\mathcal{A}^{\pm}\Delta\vec{Q}_{cv,1} + (1-\beta)\mathcal{A}^{\pm}\Delta\vec{Q}_{cv,0}. \tag{3.10}$$

A complication arises if the interface between cells is not continuous. In that case, depicted in Figure 1, in addition to the liquid/liquid and gas/gas Riemann problems, a mixed gas/liquid Riemann problem arises. For well-resolved interfaces, i.e., interfaces with local radii of curvature larger than the local control volume spacing, the face area fraction associated with the mixed Riemann problem is small and we will approximate its contribution by an incomplete two-phase Riemann solver using only the contact wave, with the left and right states approximated using the fluctuations of the single-phase Riemann problems. To achieve this, the liquid face area fraction β used in Eq. (3.10) is calculated as the average of the left and right cells' values, $\beta = (\beta^L + \beta^R)/2$, and the phase interface segment coinciding with the cell face is transported geometrically using the VoF method.

An important consequence of using average fluctuations calculated from single-phase Riemann problems, Eq. (3.10), to directly update the cell averages of mixed cells is the inherent assumption that the single-phase waves originating from cell faces do not further interact with the phase interface itself within a single time step (see panel in Figure 2 for an example). This linearization proposed by LeVeque & Shyue (1995) for wave interactions is in essence a large time step generalization (LeVeque 1985). Numerical tests, however, have shown that this linearization is viable only if the two fluids on either side of the phase interface are of comparable stiffness; i.e., p_∞ in Eq. (2.3) for both fluids

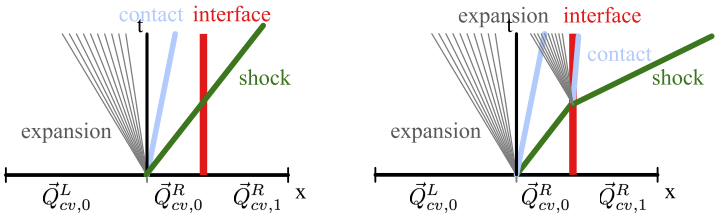

FIGURE 2. Linearized wave interaction (left) and full interface/wave interaction (right).

is similar. For liquid/gas systems, the interaction of waves originating from the cell-face Riemann problems with the phase interface has to be taken into account (LeVeque & Shyue 1995; Shyue 1993).

For this purpose we have developed an exact two-phase Riemann solver following the procedure by Kamm (2015) that allows for an arbitrary jump in the equation of state. If within a time step it is detected that a wave from the single-phase cell-face Riemann problems passes over the interface, a new two-phase Riemann problem at the phase interface is solved, with the reconstructed state of one phase modified by the incoming wave on one side and the reconstructed state of the other phase on the other side. In the example shown in Figure 2, the left state of the two-phase Riemann problem is $\vec{Q}^R_{cv,0} - \mathcal{W}^3_0$ and the right state is $\vec{Q}^R_{cv,1}$, assuming that the $p = 3$ wave is the shown shock originating from the gas-phase Riemann problem at the cell face. Note that within a single time step, only shocks or expansion waves can interact with the interface, since contact waves propagate with the same speed as the interface.

The interface two-phase Riemann problem results in three waves $\mathcal{W}^{*,p}$ and associated fluctuations. To take these properly into account, we modify Eq. (3.2) according to

$$\mathcal{A}^{\pm}\Delta\vec{Q} = \sum_p \delta^p (\lambda^p)^{\pm} \mathcal{W}^p + \sum_p \delta^{p*} (\lambda^{*,p})^{\pm} \mathcal{W}^{*,p}, \tag{3.11}$$

where δ^p is

$$\delta^p = \begin{cases} \frac{\Delta t^p}{\Delta t} & : \text{ if wave } p \text{ passes over interface} \\ 1 & : \text{ if wave } p \text{ does not pass over interface} \end{cases} \tag{3.12}$$

with Δt^p as the time it takes wave p to reach the phase interface, and

$$\delta^{p*} = \begin{cases} \frac{\Delta t^{p*}}{\Delta t} & : \text{ if wave } p^* \text{ passes over interface} \\ 1 & : \text{ if wave } p^* \text{ does not pass over interface} \end{cases} \tag{3.13}$$

with Δt^{p*} as the time it takes wave p^* to reach the cell face again. If wave p^* passes the cell face into the neighboring cell, the update for that cell has to be modified with the remainder of the wave contribution, i.e., $\sum_p (1 - \delta^p - \delta^{p*})(\lambda^{*,p})^{\pm} \mathcal{W}^{*,p}$. Note that the proposed interaction scheme assumes that waves within the same phase interact linearly and can be superposed; i.e., the large time step generalization of LeVeque (1985) is applicable in the single-phase regions. In the numerical experiments performed in this report, we have found this assumption to be reasonable.

Finally, for the purposes of setting up the two-phase Riemann problem at the phase interface and to calculate the interaction times Δt^p and Δt^{p*}, we assume that the interface is parallel to the cell face in question, with the distance of the interface to the cell face given by the respective volume fractions α or $1 - \alpha$. Note that for the purposes of the wave interaction only, this is in essence the SLIC interface reconstruction of VoF methods (Noh & Woodward 1976).

3.3. *Interface wave*

In the wave propagation scheme, the phase interface itself is a wave and must be taken into account. The motion of the interface wave is given by the solution to the volume fraction equation, Eq. (2.7). We solve it using an extension of the geometric framework proposed by Owkes & Desjardins (2014).

We need to calculate the wave contribution of the phase interface wave to the change in the volume averaged conservative variables, i.e.,

$$\Delta\vec{Q}_{cv} = \sum_n \frac{\alpha^n_{0,0}\Omega^n_{0,0} - (1-\alpha^n_{1,1})\Omega^n_{1,1} + \alpha^n_{0,1}\Omega^n_{0,1} - (1-\alpha^n_{1,0})\Omega^n_{1,0}}{V_{cv}}(\vec{Q}^n_1 - \vec{Q}^n_0) \\ -\frac{\Omega_{0,1}}{V_{cv}}(\vec{Q}^R_{cv,1} - \vec{Q}^L_{cv,0}) + \frac{\Omega_{1,0}}{V_{cv}}(\vec{Q}^L_{cv,1} - \vec{Q}^R_{cv,0})\,. \tag{3.14}$$

Here, $\Omega^n_{0,0}$, $\Omega^n_{1,1}$, $\Omega^n_{1,0}$, and $\Omega^n_{0,1}$ are portions of the flux volumes originating from the cell-face portion that on either side of the face is gas/gas, liquid/liquid, liquid/gas, or gas/liquid, and is within a neighbor cell n that is intersected by the respective flux volumes, with $\alpha^n_{0,0}$, $\alpha^n_{1,1}$, $\alpha^n_{1,0}$, and $\alpha^n_{0,1}$ the liquid volume fractions in the respective flux volume portions. Similarly, $\Omega_{1,0}$ and $\Omega_{0,1}$ are the entire flux volume portions, uncut by neighboring cells, see Figure 1. The flux volume portions and corresponding liquid volume fractions are calculated using the geometric framework of Owkes & Desjardins (2014), which is applied to the face area fractions that have the corresponding phases on either side. The corresponding vertices are followed backward in time using a Lagrangian technique with interpolated face-normal velocities that are set to the contact discontinuity speed of the corresponding face Riemann problem built with the reconstructed states. The necessary correction volume for the overall face flux volume is calculated following the procedure of Owkes & Desjardins (2014); however, the correction volume is split among the individual flux volume portions according to the volume fraction of the flux volume portion; e.g., the fraction of the correction volume Ω_{corr} associated to the $\Omega_{0,0}$ flux volume portion is $\Omega_{corr}\Omega_{0,0}/(\Omega_{0,0}+\Omega_{1,1}+\Omega_{1,0}+\Omega_{0,1})$.

The resulting scheme to solve the left-hand side of Eq. (2.7) is still unsplit, conservative, and bounded. However, unlike in incompressible flows, the volume of each phase is not conserved, resulting in the source term on the right-hand side of Eq. (2.7). Since the jump in velocities across the phase interface is zero (see Eq. (2.5)), the source term is evaluated with Gauss theorem using the face-normal velocities.

4. Results

4.1. *1-D shock in air impacting an air/water interface*

The first verification problem consists of a Ma = 3 shock in air impacting an air/water phase interface. The shock is placed initially at $x = 0.2$ inside a unit sized domain, with the air/water phase interface located at $x = 0.3$. The initial conditions are to the left of the shock $(\rho, u, p, \gamma, p_\infty)^L_0 = (0.462857, 0.240027, 0.103333, 1.4, 0)$, to the right of the shock $(\rho, u, p, \gamma, p_\infty)^R_0 = (1.2, 0, 1, 1.4, 0)$, and in the water $(\rho, u, p, \gamma, p_\infty)_1 = (1000, 0, 1, 5.5, 4921.15)$. A mesh of 400 equidistant cells is used with CFL = 0.5.

Figure 3 compares the computed density and pressure solution with the exact solution at three different instances in time. The computed solution is in excellent agreement with the exact solution, which consists of both reflected and transmitted shocks. The phase interface remains a discontinuity without any visible pressure oscillations. Although the transmitted shock in the liquid exhibits a strong pressure jump, the associated density

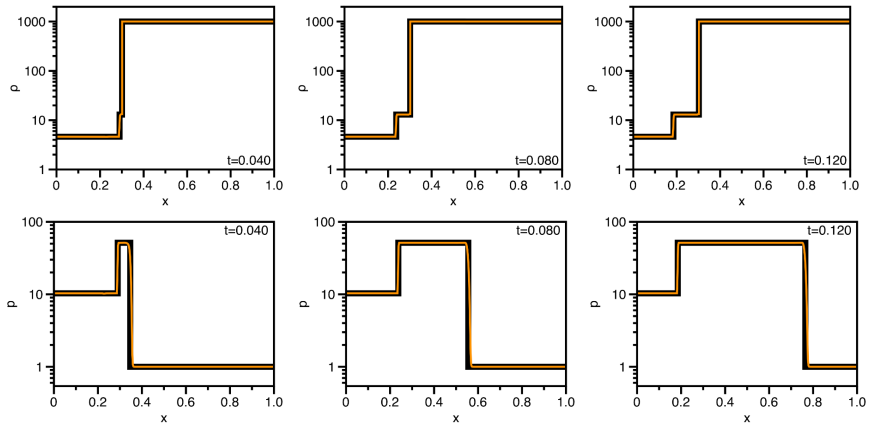

FIGURE 3. Density (top) and pressure (bottom) solutions at $t = 0.04$, 0.08, and 0.12 time units for shock in air impacting an air/water interface using log-scale; exact solution (thick black line), computed solution (thin orange line). Both lines are practically indistinguishable (see online color version).

jump is practically invisible in the density solution due to the high stiffness in the equation of state for water.

4.2. *2-D shock/drop interaction*

A shock at Ma = 1.22 in air impacts a collection of 13 water drops. The computational domain is a 0.4 by 0.2 rectangular box. The pre-shock conditions in the air are $(\rho, u, p, \gamma, p_\infty)_0 = (1, 0, 1, 1.4, 0)$ and in the water are $(\rho, u, p, \gamma, p_\infty)_1 = (1000, 0, 1, 5.5, 4921.15)$. Surface tension is neglected in this case. The drops are randomly placed, with centers from 0.115 to 0.22 from the left boundary and random radii between 0.008063 and 0.0127. The shock is placed initially at 0.1 units from the left boundary. Simulations are carried out for a coarse mesh of 200 by 100 equidistant cells in order to test how the scheme performs if the water drops are resolved by only 4 to 6 points per radius.

Figure 4 shows numerical Schlieren images of the simulation results at different times. Note that the liquid/gas phase interface appears smeared over several cells. This is merely an artifact of the post-processing done in ParaView to obtain the numerical Schlieren image and the used coarse resolution. The actual sharp phase interface location is indicated by thin orange lines. As shown, the shock wave passing over the drop cloud is partially reflected and transmitted very weakly through the drops. Reflected and transmitted waves show a complex interaction pattern. The drops start to move and, due to the lack of surface tension, begin to deform. Upon close examination, barely visible weak acoustic waves that are due to the SLIC-type treatment of the wave/interface interaction scheme can be discerned within the drops. A PLIC-type treatment would avoid these waves and should be pursued in the future.

5. Conclusions

We have presented a hybrid capturing/tracking method for compressible multiphase flows that couples an unsplit geometric volume tracking method with a finite volume wave propagation scheme. In cells containing the phase interface, states on either side of the interface are reconstructed such that the cell-face Riemann problems can be solved

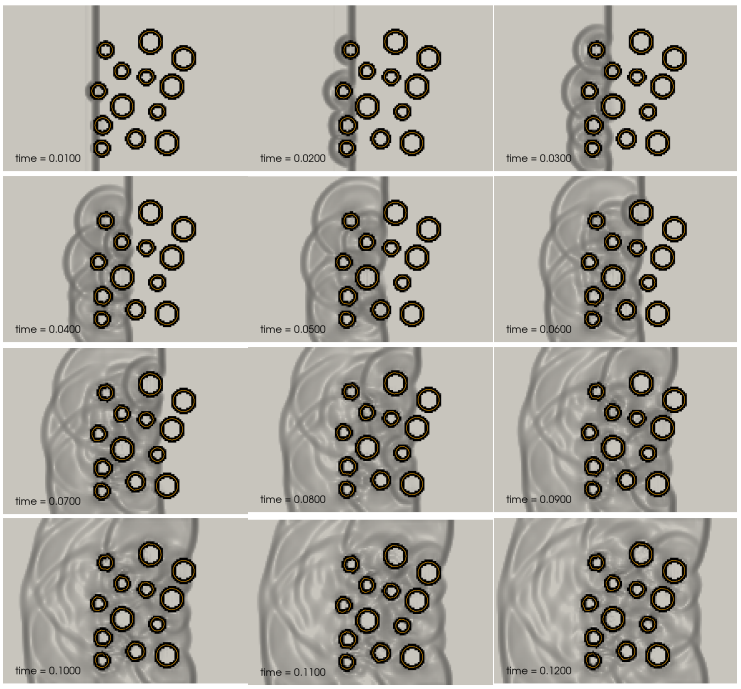

FIGURE 4. Numerical Schlieren images of a Ma = 1.22 shock in air impacting water drops. Log-scale for density gradient magnitude ranging from 1 to 10,000. Times shown from top left to bottom right are from $t = 0.01$ to 0.12 every 0.01. Thin orange line is the reconstructed interface location.

within each phase separately. Using area-fraction-weighted single-phase fluxes together with a linearization of the wave interaction across cell faces avoids the small cut-cell time step limitation of typical tracking methods. The interaction of waves with the phase interface is solved using an exact two-phase Riemann solver with arbitrary jumps in the equation of state.

Future work will focus on extending the proposed method to three dimensions and to replace the SLIC-type wave interface interaction with a PLIC-type interaction.

REFERENCES

Bo, W. & Grove, J. W. 2014 A volume of fluid method based ghost fluid method for compressible multi-fluid flows. *Comput. Fluids* **90**, 113–122.

Bo, W., Liu, X., Glimm, J. & Li, X. 2011 A robust front tracking method: verification and application to simulation of the primary breakup of a liquid jet. *SIAM J. Sci. Comput.* **33**, 1505–1524.

Chern, I. L., Glimm, J., McBryan, O., Plohr, B. & Yaniv, S. 1986 Front tracking for gas dynamics. *J. Comput. Phys.* **62**, 83–110.

Fedkiw, R., Aslam, T., Merriman, B. & Osher, S. 1999 A non-oscillatory Eulerian approach to interfaces in multimaterial flows (the ghost fluid method). *J. Comput. Phys.* **152**, 457–492.

Glaister, P. 1988 An approximate linearised Riemann solver for the three-dimensional Euler equations for real gases using operator splitting. *J. Comput. Phys.* **77**, 361–383.

Grund, F. 1979 Forsythe, G. E. / Malcolm, M. A. / Moler, C. B., Computer Methods for Mathematical Computations. Englewood Cliffs, New Jersey 07632. Prentice Hall, Inc., 1977. XI, 259 S. *ZAMM-Z. Angew. Math. Me.* **59**, 141–142.

Harten, A. & Hyman, J. M. 1983 Self adjusting grid methods for one-dimensional hyperbolic conservation laws. *J. Comput. Phys.* **50**, 235–269.

Hu, X. Y., Khoo, B. C., Adams, N. A. & Huang, F. L. 2006 A conservative interface method for compressible flows. *J. Comput. Phys.* **219**, 553–578.

Jemison, M., Sussman, M. & Arienti, M. 2014 Compressible, multiphase semi-implicit method with moment of fluid interface representation. *J. Comput. Phys.* **279**, 182–217.

Kamm, J. R. 2015 *An exact, compressible one-dimensional Riemann solver for general, convex equations of state*. Tech. Rep. LA - UR - 15 - 21616.

Langseth, J. O. & LeVeque, R. J. 2000 A wave propagation method for three-dimensional hyperbolic conservation laws. *J. Comput. Phys.* **165**, 126–166.

van Leer, B. 1977 Towards the ultimate conservative difference scheme. IV. A new approach to numerical convection. *J. Comput. Phys.* **23**, 276–299.

LeVeque, R. J. 1985 A large time step generalization of Godunov's method for systems of conservation laws. *SIAM J. Numer. Anal.* **22**, 1051–1073.

LeVeque, R. J. 2010 *Finite Volume Methods for Hyperbolic Problems*. Cambridge University Press.

LeVeque, R. J. & Shyue, K. M. 1995 One-dimensional front tracking based on high-resolution wave-propagation methods. *SIAM J. Sci. Comput.* **16**, 348–377.

Menikoff, R. 2007 Empirical equations of state for solids. In *Shock Wave Science and Technology Reference Library* (ed. Y. Horie), pp. 143–188.

Noh, W. & Woodward, P. 1976 SLIC (simple line interface calculation). In *Proc. 5th Int. Conf. Fluid Dyn.*, ed. A. van de Vooren & P. Zandbergen, pp. 330–340. Berlin: Springer-Verlag.

Owkes, M. & Desjardins, O. 2014 A computational framework for conservative, three-dimensional, unsplit, geometric transport with application to the volume-of-fluid (VOF) method. *J. Comput. Phys.* **270**, 587–612.

Roe, P. L. 1981 Approximate Riemann solvers, parameter vectors, and difference schemes. *J. Comput. Phys.* **43**, 357–372.

Shyue, K.-M. 1993 *Front tracking methods based on wave propagation*. PhD thesis, University of Washington.

Shyue, K.-M. 1999 A volume-of-fluid type algorithm for compressible two-phase flows. In *Hyperbolic Problems: Theory, Numerics, Applications*, pp. 895–904. Birkhäuser Basel.

Smiljanovski, V. 1996 *Ein numerisches Verfahren zur Berechnung schneller Vormischflammen und der Deflagrations-Detonations-Transition (DDT)*. PhD thesis, RWTH Aachen.

Smiljanovski, V., Moser, V. & Klein, R. 1997 A capturing-tracking hybrid scheme for deflagration discontinuities. *Combust. Theor. Model.* **1**, 183–215.

Terashima, H. & Tryggvason, G. 2009 A front-tracking/ghost-fluid method for fluid interfaces in compressible flows. *J. Comput. Phys.* **228**, 4012–4037.